LEPTON PAIR PRODUCTION IN TAGGED $\gamma\gamma$ COLLISIONS AT THE L3 EXPERIMENT

EMANUELE LEONARDI
Physics Dept., "La Sapienza" University and I.N.F.N. Rome
Piazzale Aldo Moro 5, 00185 Roma, Italy
E-mail: leonardi@roma1.infn.it

ABSTRACT

We studied lepton pair production in single-tagged $\gamma\gamma$ events using the L3 detector at LEP. A measurement of the process cross section is given for $1.4\,\mathrm{GeV}^2 < Q^2 < 7.6\,\mathrm{GeV}^2$ and $60\,\mathrm{GeV}^2 < Q^2 < 140\,\mathrm{GeV}^2$. The F_2 photon structure function is then extracted at $<Q^2>= 1.7\,\mathrm{GeV}^2$. Finally a study of azimuthal correlations is used to gain access to some so far unmeasured photon structure functions.

1. Introduction

The study of the $e^+e^- \to e^+e^-\ell^+\ell^-$ processes, where ℓ can be any charged lepton, at LEP energies gives direct access to $O(\alpha^4)$ reactions. The tree level Feynman diagrams involved in the process can be classified as *multiperipheral, bremsstrahlung, annihilation,* and *conversion* [1].

In this paper we report on the results obtained with the L3 detector by studying the $e^+e^-\mu^+\mu^-$ final state when one of the two electrons goes undetected (untagged) along the beam pipe and the other one is detected (tagged) by one of the forward detectors (single-tag events). In this configuration contributions from graphs other than the multiperipheral one or from Z° exchange can be safely neglected in the description of the process. All the theoretical formulæ can then be obtained from pure QED computations [2].

In addition, as the scattering angle of the undetected electron is small (<30 mrad in L3), the photon emitted is *quasi-real.* The process is therefore equivalent to a deep inelastic scattering process in which the inner structure of the *quasi-real* photon is "probed" by the *virtual* photon emitted from the tagged electron.

If one denotes as p_1 the four-momentum of the *virtual* photon and as p_2 that of the *quasi-real* one, the differential cross section of the process can be written as

$$\frac{d^3\sigma}{dx dQ^2 dx_2} = \frac{4\pi\alpha^2}{Q^4 x}\frac{dn(x_2)}{dx_2}\{(1-y)F_2(x,Q^2) + xy^2F_1(x,Q^2)\} \qquad (1)$$

where $Q^2 = -p_1^2$, $x_{1,2} = E_{1,2}/E_{\mathrm{beam}}$, $y \simeq x_1$, $dn(x_2)/dx_2$ is the *quasi-real* photon flux[3], and $F_{1,2}(x,Q^2)$ are the photon structure functions. x is the Bjorken scaling variable which can be expressed in terms of W, the invariant mass of the final state lepton pair, as $x = \frac{Q^2}{Q^2+W^2}$.

Given the selection cuts used in this analysis, explained later, the value of y can never exceed 0.2, thus reducing to a few percent the contribution due to the F_1 structure function.

By neglecting terms of the order of $2m_\mu$ with respect to W, the F_2 structure function can be written[4] as

$$F_2(x,Q^2) = \frac{\alpha}{\pi}x\left\{[1-2x(1-x)]\ln\frac{W^2}{m_\mu^2+x(1-x)P^2} - 1 + 8x(1-x) - \frac{x(1-x)P^2}{m_\mu^2+x(1-x)P^2}\right\} \quad (2)$$

where $P^2 = -p_2^2$ is the *quasi-real* photon virtual mass. The contribution due to P^2 not being exactly equal to zero reduces the F_2 value by about 10%.

2. The L3 detector

A detailed description of the L3 detector can be found elsewhere[5]. Only the components of the detector relevant for the present analysis are briefly described here.

The position and momentum of charged particles are measured by a Time Expansion Chamber (TEC), covering the polar angle region of $13^\circ < \theta < 167^\circ$ and the full azimuthal range. The TEC momentum resolution is $\Delta p_t/p_t = 0.018 p_t(\mathrm{GeV}) + 0.02$.

The energy and position of the electromagnetic showers are measured by an homogeneous calorimeter made of Bismuth Germanium Oxide (BGO) crystals. About 11000 crystals are arranged in a *Barrel* ($42^\circ < \theta < 138^\circ$) and two *Endcap* regions ($11.6^\circ < \theta < 38^\circ$, $142^\circ < \theta < 168.4^\circ$) ensuring a fine granularity and a large acceptance for the detector. The energy resolution goes from $\simeq 5\%$ for $E = 100$ MeV to $\simeq 1\%$ for $E = 45$ GeV.

Outside the BGO barrel and endcap calorimeters, a depleted Uranium sampling calorimeter covers 99.5 % of the full solid angle ensuring the detection of hadrons and muons with a momentum $P > 1$ GeV/c.

Along the beam-pipe, about 2.7 m away from the interaction point, two cylindric BGO calorimeters, the *Luminosity monitors*, allow the measurement of electrons in the low θ region ($1.7^\circ < \theta < 3.6^\circ$) with an energy resolution of $\sigma(E)/E = 1.7\%$ for $E = 45$ GeV and a spatial resolution of $\simeq 1$ mm.

The $\gamma\gamma$ events with the *tag* particle detected in the luminosity monitors are collected by a special trigger requiring an energy deposit larger than 30 GeV in the luminosity monitor and at least one track in the TEC chamber with a transverse momentum $p_t > 100$ MeV/c (TEC+LUMI trigger). Events with a *tag* particle with

more than 8 GeV going in the endcaps are collected by an energy based trigger[6].

3. Event selection

The presence of a *tag* particle is ensured by requiring one (and only one) large deposit of energy (E > 35 GeV) in the fiducial volume either of the luminosity monitor (27 mrad $< \theta <$ 64 mrad) or of the BGO endcap (200 mrad $< \theta <$ 600 mrad). Then two tracks, none of which associated with the *tag* particle, are searched for in the TEC fiducial region $28^\circ < \theta < 152^\circ$. Finally, as a check for the existance of an electron going unseen along the beam-pipe, we require a total missing longitudinal momentum greater than 30 GeV.

The event is classified as $e^+e^-\mu^+\mu^-$ if the calorimetric information associated with at least one of the two tracks is compatible with a *minimum ionizing particle* (mip) both in the BGO and in the Uranium calorimeter.

These selection criteria were applied to the data collected from the L3 experiment from 1991 to 1993. The total integrated luminosity, limited by the operational time of the TEC+LUMI trigger, is 33.2 pb^{-1}.

For MonteCarlo studies we produced a sample of $e^+e^-\mu^+\mu^-$ events corresponding to an integrated luminosity of $\simeq 38\,pb^{-1}$. We used the DIAG36 generator program[7] which takes into account all the Feynman graphs involved in the process. Initial state radiation effects were not included in the generation process.

As a crosscheck, the request for mip-likeness of one of the tracks was replaced with the request of the track being compatible with an electron, thus selecting $e^+e^-e^+e^-$ final states.

Results for both $e^+e^-\mu^+\mu^-$ and $e^+e^-e^+e^-$ selections are shown in table 1 together with the main background sources and the MonteCarlo expectations [a].

Process	Region	Selected events	Background eeee	Background $ee\tau\tau$	Final selection	Expected from MC
$ee\mu\mu$	LUMI	2727	66±5	29±3	2632±53	2776±49
$ee\mu\mu$	ECAP	36	—	—	36±6	28±5
eeee	LUMI	1430	—	13±2	1417±38	1336±87
eeee	ECAP	6	—	—	6±2	11±8

Table 1: Selection results and MC expectations for $e^+e^-\mu^+\mu^-$ and $e^+e^-e^+e^-$ events.

4. Results

Taking into account the selection efficiencies as obtained from MC, we extracted

[a] For the $e^+e^-e^+e^-$ channel the MC statistics corresponds to $\simeq 6\,pb^{-1}$ only.

from the selected events the distribution of the cross section of the process as a function of x and Q^2. Fig. 1(a) shows a comparison of the experimental cross section with that obtained from MonteCarlo in the LUMI region while figure 1(b) shows a comparison with the curve obtained from Eq. 1 for both LUMI and ECAP.

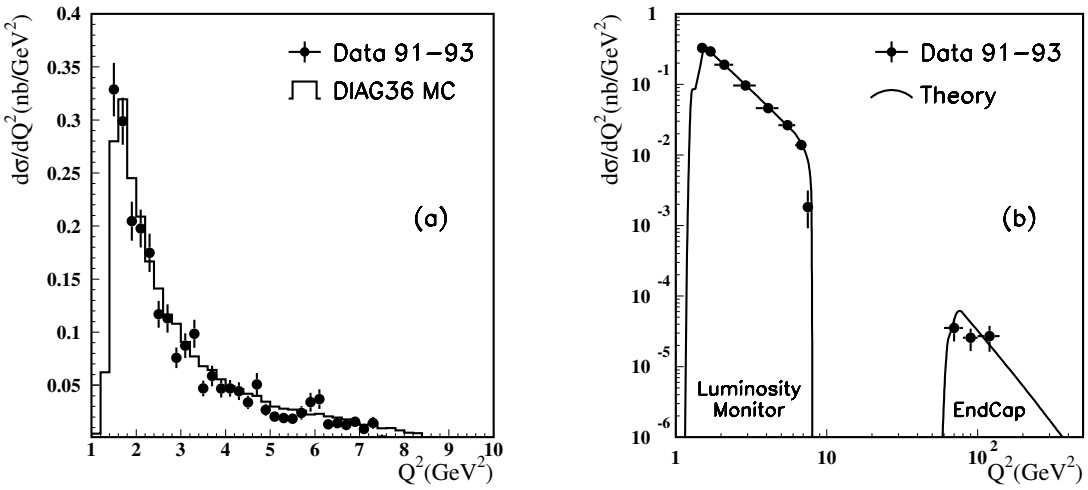

Figure 1: Cross section distribution as function of Q^2: LUMI only (a) and LUMI plus ECAP (b).

Once the cross section distribution is known in terms of x and Q^2, one can extract the value of $F_2(x, Q^2)$ in the range 1.4 GeV$^2 < Q^2 <$ 7.6 GeV^2 ($< Q^2 >$= 1.7 GeV^2), corresponding to the LUMI region. The result is shown in Fig. 2.

Several authors[7,8,9] have shown that the angular distributions of the final state leptons in the $\gamma\gamma$ system center of mass frame give access to other structure functions beside F_2.

In particular, from single-tagged events one can extract a total of three structure functions by studying the behavior of the cross-section in terms of ϕ_a, the angle between the plane defined by the two leptons axis and the two photons axis and that defined by the tagged electron and the two photon axis, everything computed in the $\gamma\gamma$ system center of mass frame.

The differential distribution of the cross-section can be written as

$$\frac{d^3\sigma}{dxdyd\Omega} = \frac{4\pi\alpha^2}{Q^4}[1 + (1-y)^2][A_1 + A_2\cos(\phi_a) + A_3\cos(2\phi_a)] \qquad (3)$$

where the terms A_1, A_2, and A_3 are proportional to the structure functions F_1, F_2, and F_3 described by Kessler[9] and depend on x and on $z = cos\theta$, θ being the angle between the leptons and the photons axes.

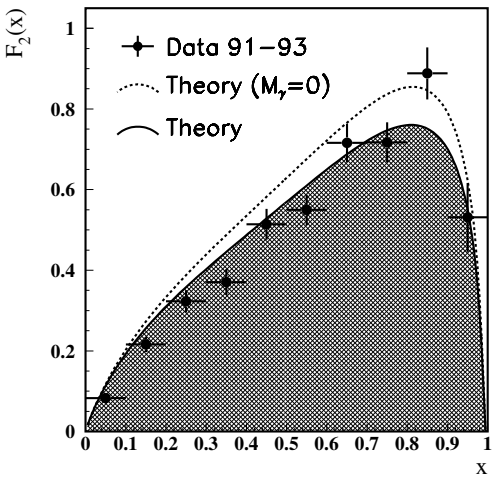

Figure 2: Value of $F_2(x)$ measured in the range $1.4\ \text{GeV}^2 < Q^2 < 7.6\ \text{GeV}^2$ ($< Q^2 >= 1.7\ \text{GeV}^2$). The effect of the *quasi-real* photon mass is also shown.

Experimentally, we measured the number of events in four ranges of x and z as a function of ϕ_a, correcting them with the MonteCarlo to take into account the incomplete coverage for outgoing muons of our detector.

The chosen x and z ranges were $0 < x < 0.5$ or $0.5 < x < 1$ and $-0.8 < z < 0$ or $0 < z < 0.8$. The z ranges do not extend up to ± 1 as in this configuration, i.e. leptons emitted collinearly to the photons, the sharp peak in the F_1 structure function would completely hide the effect of F_2 and F_3.

These distributions were then fitted with the function

$$\frac{d\sigma}{d\phi_a} = K[1 + A\cos(\phi_a) + B\cos(2\phi_a)] \tag{4}$$

were K is a normalization factor while A and B are defined as

$$A = \frac{\int_{\Delta x}\int_{\Delta z} A_2(x,z)dxdz}{\int_{\Delta x}\int_{\Delta z} A_1(x,z)dxdz} \qquad \text{and} \qquad B = \frac{\int_{\Delta x}\int_{\Delta z} A_3(x,z)dxdz}{\int_{\Delta x}\int_{\Delta z} A_1(x,z)dxdz} \tag{5}$$

Figure 3 shows the ϕ_a distribution for the chosen x and z ranges together with the fitted curves while table 2 shows the result of the fits compared to the value expected from the theory.

5. Developments for LEP II

At the end of 1994 L3 installed a new detector, the Active Lead Ring[10] (ALR), which covers the gap between the luminosity monitor and the electromagnetic calorimeter endcap (68 – 140 mrad). In addition, at the end of 1995 another detector will be

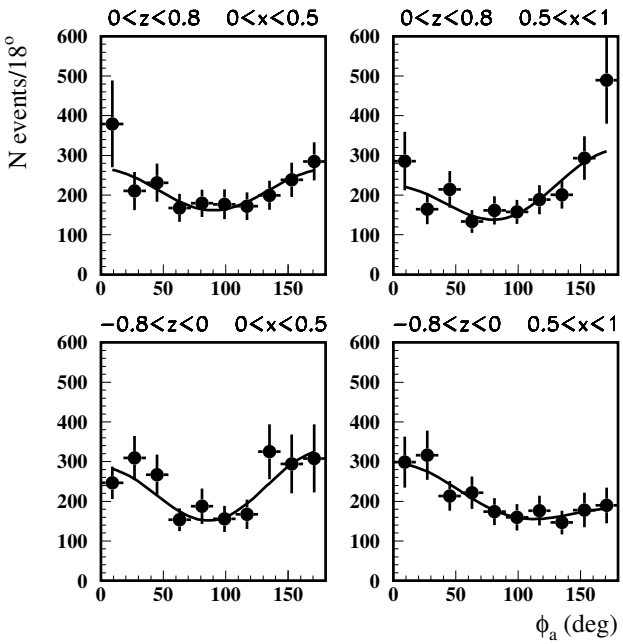

Figure 3: Angular distributions for the x and z ranges described in the text

Ranges		Experiment		Theory	
Δx	Δz	A	B	A	B
0 – 0.5	0 – 0.8	0.00 ± 0.10	0.24 ± 0.09	0.15	0.22
0.5 – 1	0 – 0.8	-0.22 ± 0.11	0.31 ± 0.09	-0.19	0.17
0 – 0.5	-0.8 – 0	-0.09 ± 0.11	0.34 ± 0.09	-0.15	0.22
0.5 – 1	-0.8 – 0	0.28 ± 0.10	0.18 ± 0.09	0.19	0.17

Table 2: Azimuthal correlations: fit results and theory comparison for the chosen x and z ranges

Detector	Range (mrad)	Q^2 range (GeV^2)	
		LEP I	LEP II
VSAT	4.6 – 10.2	—	0.2 – 0.8
LUMI	30 – 62	1.4 – 7.6	7 – 31
ALR	68 – 140	7.3 – 40	36 – 160
ECAP	200 – 600	60 – 710	332 – 3440

Table 3: L3 angular and Q^2 coverage for electron tagging

installed in the very forward region of experiment: the Very Small Angle Tagger[11] (VSAT) which will cover the range between 5 and 10 mrad.

In total, when LEP will enter its second phase, L3 will be able to cover the whole angular range starting at 5 mrad from the beam axis, as shown in table 3. This, added to the increased cross section for $\gamma\gamma$ processes, would allow a complete study of single- and double-tag events, thus providing a measure of a full set of photon structure functions.

6. Acknowledgments

I wish to thank all members of the L3 two-photon group for helpful discussions and in particular Dr. B. Bertucci, Dr. J.H. Field, Prof. M.N. Kienzle-Focacci, and Dr. N. Produit for their contribution to this work.

7. References

1. F.A. Berends, P.H. Daverveldt, and R. Kleiss, *Nucl. Phys.* **B253** (1985) 421
2. V.M. Budnev *et al.*, *Phys. Rep.* **15C** (1975) 181
3. Ch. Berger and J.H. Field, *Nucl. Phys.* **B187** (1981) 585
4. CELLO Collab., H.J. Behrend *et al.*, *Phys. Lett.* **126B** (1983) 384
5. L3 Collab., B. Adeva *et al.*, *Nucl. Inst. Meth.* **A289** (1990) 35
6. R. Bizzarri *et al.*, *Nucl. Inst. Meth.* **A317** (1992) 463
   P. Bagnaia *et.al.*, *Nucl. Inst. Meth.* **A323** (1992) 528
7. F.A. Berends, P.H. Daverveldt, and R. Kleiss, *Comp. Phys. Comm.* **40** (1986) 285
8. C. Peterson, F.M. Zerwas, T.F. Walsh, *Nucl. Phys.* **B229** (1983) 301
9. CELLO Collab., H.J. Behrend *et al.*, *Z. Phys.* **C43** (1989) 1
10. P. Kessler, same proceedings
11. B. Bertucci *et al.*, L3 internal note 1504, September 3, 1993
12. G.J Bobbink *et al.*, L3 internal note 1682, December 2, 1994